

Supporting Information

X-ray Magnetic Circular Dichroism Spectroscopy Applied to Nitrogenase and Related Models: Experimental Evidence for a Spin-Coupled Molybdenum(III) Center

*Joanna K. Kowalska, Justin T. Henthorn, Casey Van Stappen, Christian Trncik, Oliver Einsle, David Keavney, and Serena DeBeer**

anie_201901899_sm_miscellaneous_information.pdf

Supporting Information

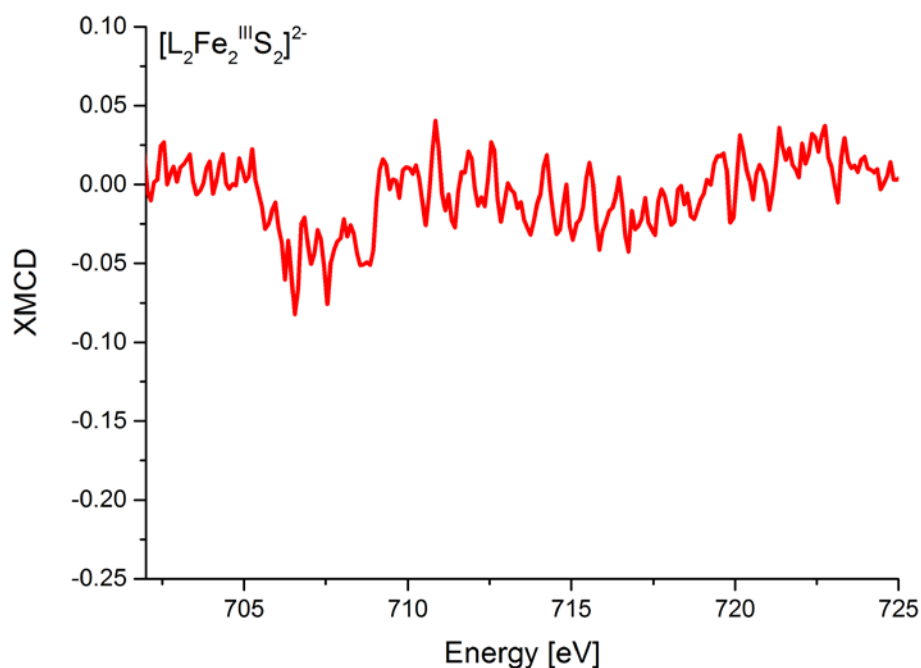


Figure S1. Experimental Fe XMCD spectra of $[L_2Fe_2S_2]^{2-}$ (adapted with permission from J.K. Kowalska, B. Nayyar, J.A. Rees, C.E. Schiewer, S.C. Lee, J.A. Kovacs, F. Meyer, T. Weyhermüller, E. Otero, S. DeBeer (2017). Iron $L_{2,3}$ -edge X-ray Absorption and X-ray Magnetic Circular Dichroism Studies of Molecular Iron Complexes with Relevance to the FeMoco and FeVco Active Sites of Nitrogenase *Inorganic Chemistry* 56, 8147-8158. Copyright (2017) American Chemical Society.)

Materials & Methods

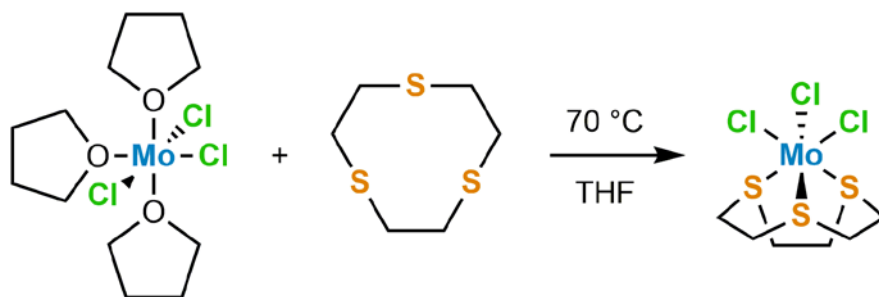
I. General considerations:

Unless indicated otherwise, all reactions were conducted using oven-dried glassware in a nitrogen-filled glovebox or on a Schlenk line using standard Schlenk techniques. THF was purchased anhydrous from Sigma, vacuum distilled from sodium benzophenone ketyl and stored over 4 Å molecular sieves prior to use.

Elemental analysis was conducted by Mikrolab Kolbe (Mülheim an der Ruhr, Germany).

Unless indicated otherwise, all reagents were purchased from commercial sources and used as received. 1,4,7-trithiacyclonane was purchased from Sigma. $MoCl_3(THF)_3$ was prepared according to literature procedure.¹

II. Synthesis of molybdenum(III) (1,4,7-trithiacyclonane)chloride, $Mo^{III}(tten)Cl_3$



Scheme 1.

MoCl₃(THF)₃ (0.2294 g, 0.548 mmol) and 1,4,7-trithiacyclononane (0.1125 g, 0.624 mmol) were combined in THF (10 mL) and added to a Schlenk tube charged with a stir bar and fitted with a screw-in Teflon stopper. The sealed vessel was removed from the glovebox and heated to 70 °C with stirring in an oil bath for 4 hours, resulting in the formation of an orange precipitate and a colorless supernatant. After cooling to room temperature, the Schlenk tube was brought back into the glovebox and the solid collected on a glass frit, washing with additional THF (~10 mL). The resulting solid was then dried under vacuum to yield 0.1966g (94%) of the desired product as a bright orange solid. The compound was found to be completely insoluble in all common laboratory solvents tested (Pentane, Et₂O, C₆H₆, PhMe, THF, DCM, MeCN, DMF, DMSO). Anal. Calcd for (Mo^{III}(ttcn)Cl₃, C₆H₁₂Cl₃MoS₃: C, 18.83; H, 3.16. Found: C, 19.03; H, 3.25.

III. Magnetic Susceptibility of Mo^{III}(ttcn)Cl₃

Temperature-dependent (2-298 K) magnetic susceptibility data were recorded on a SQUID magnetometer (MPMS Quantum design) in an external magnetic field of 1T. The experimental susceptibility data were corrected for underlying diamagnetism by the use of tabulated Pascal's constants. Magnetic susceptibility data were analyzed and fit using julX2 software developed by Eckhard Bill at MPI CEC.

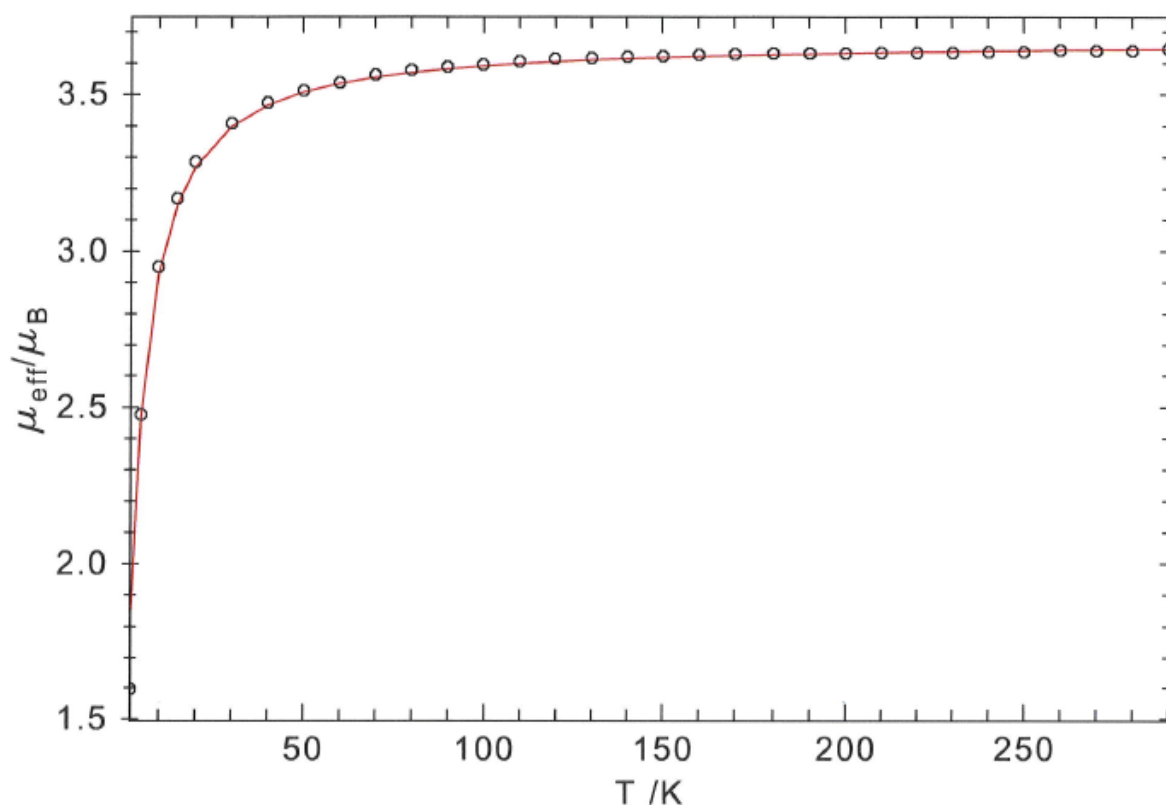

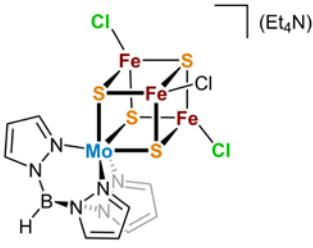
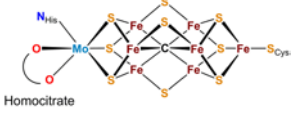


Figure S2. Plot of μ_{eff} vs. temperature for $\text{Mo}^{\text{III}}(\text{ttcn})\text{Cl}_3$ at applied field of 1T (circles). Fit to experimental data given as solid red line with the following fit parameters: $S = 3/2$, $g = 2.00$, $D = 8.5$, $E/D = 0.00$, $\chi(\text{TIP}) = 380 \times 10^{-6}$ emu (subtracted), and diamagnetic impurity of 10%.

Sample Information

Table S1. Schematic view and local spin ground state information for the molybdenum complexes used in this work; Tp = tris(pyrazolyl)borate, ttcn = 1, 4, 7 - trithiacyclononane.

Schematic view	Chemical formula	Spin			Abbreviation (used in this work)
		Total	Fe	Mo	
	$\text{Mo}^{\text{III}}(\text{ttcn})\text{Cl}_3$	$\frac{3}{2}$		$\frac{3}{2}$	$\text{Mo}^{\text{III}}(\text{ttcn})\text{Cl}_3$
	$[\text{Mo}^{\text{III}}\text{Fe}_3\text{S}_4\text{Cl}_3(\text{Tp})](\text{Et}_4\text{N})$	$\frac{3}{2}$	2	$\frac{1}{2}$	$[\text{Mo}^{\text{III}}\text{Fe}_3\text{S}_4]^{3+}$

	$[\text{Mo}^{\text{III}}\text{Fe}_7\text{S}_9\text{C}]^{1-}$	$\frac{3}{2}$	2	$\frac{1}{2}$	FeMoco
---	--	---------------	---	---------------	--------

IV. Sample preparation

The $(\text{Et}_4\text{N})[(\text{Tp})\text{Mo}^{\text{III}}\text{Fe}_3\text{S}_4\text{Cl}_3]$ (Et_4N = tetraethylammonium; Tp = tris(pyrazolyl)borate) was synthesised as reported before.² The $\text{Mo}^{\text{III}}(\text{ttcn})\text{Cl}_3$ complex (ttcn = 1,4,7-trithiacyclononane) was synthesized according to the procedure provided above. The samples were used as powders, finely ground using a mortar and pestles in an inert N_2 atmosphere glovebox. These powders were spread on carbon tape, attached to copper sample block holders and transferred to the measurement chamber *via* a helium flushed glovebag.

Mo nitrogenase was prepared as previously described.³ Lyophilization was performed on an anaerobic solution containing 27 mg/ml desalted MoFe protein, 5 mM Tris buffer ($\text{pH} = 7.5$), and 2.5 mM sodium dithionite in micropore purified, de-aerated H_2O . This procedure involves freezing the solution in liquid N_2 for approximately 30 minutes, followed by placement under vacuum for several days. This process was monitored by X-band EPR prior to lyophilization, after lyophilization, and again on lyophilized protein which had been reconstituted using a 5 mM Tris ($\text{pH} = 7.5$), 2.5 mM sodium dithionite buffer. These spectra are provided in Figure S3. Samples of lyophilized protein for XMCD measurements were prepared in an inert N_2 atmosphere glovebox by smearing the lyophilized protein powder onto a carbon tape affixed to a copper sample block, followed by transfer to the measurement chamber *via* a glovebox attached to the beamline vacuum system in case of Fe $L_{2,3}$ -edge XAS and XMCD measurements and *via* a helium purged glovebag for the Mo L_3 -edge XAS and XMCD measurements.

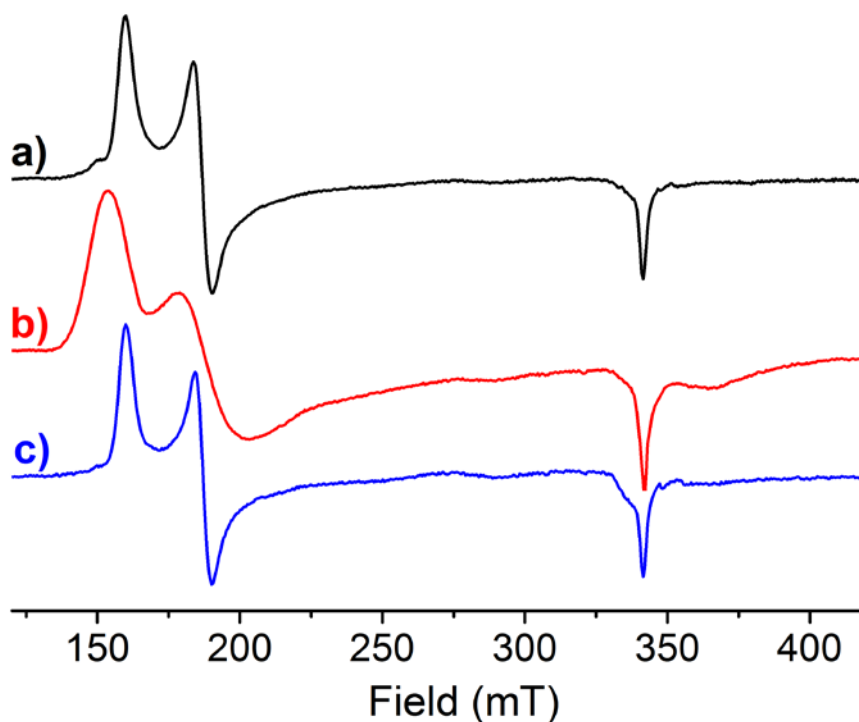


Figure S3. X-band EPR spectra of MoFe N₂ase a) prior to lyophilisation, b) as lyophilisate, and c) lyophilisate reconstituted into a 2.5 mM dithionite, 5 mM Tris solution ($\text{pH} = 7.5$). A small, broad signal

around $g = 1.88$ (~360 mT) is seen in spectrum b) due the presence of background condensed O_2 in the sample.

V. Data collection and processing

V.1 Molybdenum L_3 -edge XAS and XMCD spectroscopy of $[Mo^{III}Fe_3S_4]^{3+}$ and $Mo^{III}(ttn)Cl_3$ and MoFe protein

Molybdenum L_3 -edge (2520 eV) X-ray Absorption (XAS) and X-ray Magnetic Circular Magnetic Dichroism (XMCD) data were collected at the 4-ID-C beam line at the Advanced Photon Source (APS) facility at the Argonne National Laboratory.⁴ During the course of the measurements, the 7 GeV ring operated in a decay mode with maximum current of 102 mA. The 4-ID-C beam line utilizes a circularly polarizing undulator (CPU) as a polarized X-ray photons source and spherical grating monochromator. The polarization rate for the circular left and circular left polarized photons at this beam line at the Mo L_3 -edge energy is nearly 100%. For molybdenum L_3 -edge XAS/XMCD measurement the 1200 l/mm grating was used. During the measurements the samples were placed in a cryostat chamber under $\sim 9 \cdot 10^{-9}$ mbar vacuum, at 4 K temperature and applied ± 6 T magnetic field. The energy and intensity of the incoming polarized X-ray photons were monitored with a gold mesh, with full photocurrent transmission, while the signal coming from the samples was detected in a total electron yield mode (TEY) using a drain current. The signal coming from the MoFe protein sample was measured in total fluorescence mode using a Vortex SII detector. In order to avoid radiation-induced damage an X-ray beam size of $500 \times 500 \mu m^2$ on the sample was used. During the measurements the spectral signal was monitored for any changes due to radiation-induced damages. For both of the compounds, no radiation damage signs were observed for at least two spectra for both polarizations obtained at a fresh sample spot. This allowed to measure two sets of spectra with polarization changes (CR/CL) at every pristine spot. The Mo L_3 -edge XAS data were obtained by averaging spectra obtained with circularly right (CR) and circularly polarized left (CL) light at ± 6 T magnetic field. The Mo L_3 -edge XMCD data were obtained as a differential signal between the spectra obtained with right and left polarized light at ± 6 T magnetic field. For the $Mo^{III}(ttn)Cl_3$ complex 11 sets of CR/CL sets were used to obtain the Mo L_3 -edge and XMCD, while for the $(Et_4N)[(Tp)MoFe_3S_4Cl_3]$ complex 18 sets were used. To obtain the L_3 -edge XAS spectra of the MoFe protein presented in Figure S2, 21 sets of CR/CL spectra were averaged. The averaged spectra were background subtracted in the pre and post L_3 -edge region with a shallow 2nd order polynomial function. After that, the L_3 -edge spectra were normalized by setting the maximum of the L_3 -edge to unity. The energy of the averaged spectra was calibrated based on the S K-edge XAS spectrum of $Na_2S_2O_3 \cdot 5H_2O$ by setting the position of the lowest energy feature to 2472.0 eV.

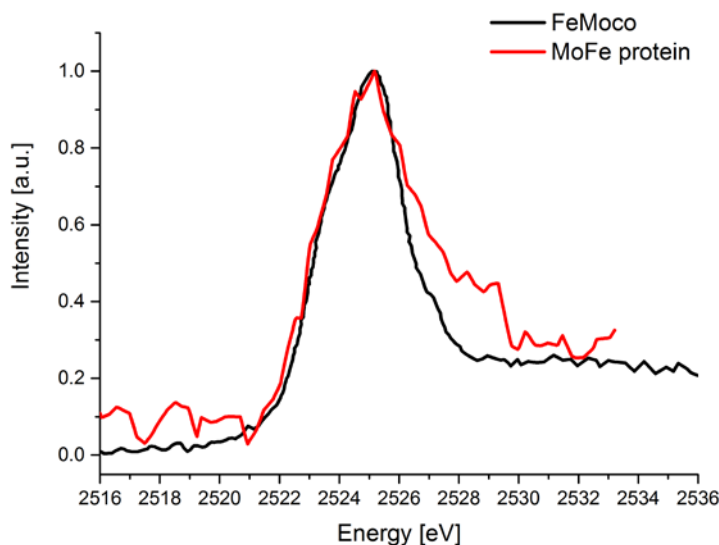


Figure S4. Normalized Mo L₃-edge XAS spectra of FeMoco (adapted with permission from reference [5], black) and MoFe protein (red).

V.2 Fe L_{2,3}-edge XAS and XMCD spectroscopy of [Mo^{III}Fe₃S₄]³⁺

Fe L_{2,3}-edge XAS and XMCD data of the [Mo^{III}Fe₃S₄]³⁺ cubane were collected as previously described.⁶ The averaged spectra were background subtracted in the pre- L₃ and post L₂-edge region with a shallow 2nd order polynomial function and normalized by setting the maximum of L₃-edge to unity. The XMCD spectra were obtained by subtracting the spectrum obtained with circularly left polarized light from the spectrum obtained with right circularly polarized light at ±6 T magnetic field. To remove all uncertainty the XMCD spectrum was corrected by subtracting the XMCD spectrum obtained at 0 T magnetic field. The XMCD data were normalized by setting the XMCD signal to unity as reported in reference [7]. The data processing was done using ATHENA.^[11]

V.3 Fe L_{2,3}-edge XAS and XMCD spectroscopy of MoFe protein

Fe L_{2,3}-edge XAS and XMCD data were collected at DEIMOS beamline at the SOLEIL synchrotron facility in France. The 2.75 eV ring operated in a top-up mode, providing a 450 mA electron current. The source of polarized photons was an APPLE II undulator equipped with a plane grating monochromator (PGM) equipped with a variable groove depth grating (VGD). The measurements were conducted in ultrahigh vacuum environment (~10⁻¹⁰ mbar), at a temperature of 4 K and either 0 T magnetic field (XAS) or ±6 T magnetic field (XMCD) utilizing a superconducting magnet⁸⁻⁹. The incoming X-rays were monitored by a photocurrent of a gold grid with 50% transmission reference monitor. The signal from the MoFe protein was detected in total fluorescence mode (TFY) using a diode. In order to avoid radiation induced damage, the beam size was set to 800 x 800 μm² and after 4 scans the beam was move to a fresh spot of the sample.¹⁰ The energy of the incoming photons was calibrated as previously reported to the spectrum of K₃[Fe(CN)₆].⁶

The L_{2,3}-edge XAS spectra were obtained by averaging the data obtained with circularly right and left polarized photons at 0T magnetic field. The spectra presented in Figure 2 (top) are an average of 110 spectra in total. The XMCD signal was obtained as a difference between spectra obtained with opposite circularly polarized photons at applied magnetic field. The signal was then corrected by subtracting the

XMCD at 0 T magnetic field. This gave 84 sets of spectra (CR/CL) with half obtained at +6 T and half with at -6 T magnetic field. The data processing was done in the same way as for the $[\text{Mo}^{\text{III}}\text{Fe}_3\text{S}_4]^{3+}$ cubane.

V.4 Mo K-edge HERFD XAS spectroscopy of $\text{Mo}^{\text{III}}(\text{ttn})\text{Cl}_3$

Mo-K α (20000 eV) high-energy resolution fluorescence detected X-ray ray absorption (HERFD-XAS) data were collected at the ID26 beamline at the European Synchrotron Radiation Facility (ESRF). The storage ring operated at 6 GeV in 16 bunch top-up mode at an approximately 90 mA ring current. A double-crystal monochromator using a pair of Si(311) crystals was employed to select the incoming X-ray energy with an intrinsic resolution ($\Delta E/E$) of 0.3×10^{-4} . The X-ray beam size was $500 \times 1000 \mu\text{m}^2$ (V x H) at the sample position. A liquid helium flow-cryostat was maintained at approximately 20 K in order to reduce the degree of radiation damage and maintain an inert sample environment.

The energy of the incoming x-rays was calibrated by recording the transmission K-edge XAS spectrum of a Mo foil and assigning the energy of the maximum of the white line to 20016.4 eV. The spectrometer was equipped with five curved Ge(111) crystals positioned at a Bragg angle of 77.74° , utilizing the [999] reflection to focus the Mo-K α_1 emission (~ 17480 eV) on the detector in a Johann-type geometry. Spectra were collected using a Ketek silicon drift detector. Individual scans were normalized to the incident photon flux and averaged using PyMCA.¹¹ Preliminary scans were performed to determine the rate of damage upon irradiation. $\text{Mo}(\text{ttn})\text{Cl}_3$ showed no signs of damage up to 150 seconds. Short X-ray absorption near-edge spectra (XANES) scans were collected by scanning the incident energy from 19990 to 20090 eV, while long extended x-ray absorption fine structure (EXAFS) scans were obtained by collection from 19990 to 20910 eV. Both XANES and EXAFS scans were collected using 120s scan times. The XANES spectrum was produced by averaging of 3 scans, while the EXAFS spectrum was produced by averaging of 47 scans.

Solid samples were prepared as powders by finely grinding $\text{Mo}(\text{ttn})\text{Cl}_3$ using a mortar and pestle, and diluting to 50% by mass using boron nitride. Further processing of spectra including background subtraction and normalization was performed using the Athena program from the software package Demeter following standard protocols for X-ray spectroscopy.¹² Background subtraction from the EXAFS spectrum was performed using a linear regression for the pre-edge region of 19910-19947 eV, and a quadratic polynomial regression for the post-edge region of 20157-20807 eV. EXAFS fitting was performed using the program Artemis, also of the software package Demeter.

The Mo K α XANES spectrum of $\text{Mo}^{\text{III}}(\text{ttn})\text{Cl}_3$ is provided in Figure S3, demonstrating a typical Mo(III) spectrum with a relatively weak pre-edge Mo 1s \rightarrow 4d feature around 20001 eV. EXAFS data, shown in Figure S4, were processed by modelling of a series of possible scenarios for Mo ligation, including full Cl or S coordination, as well as partial coordination. All fits were performed using single scattering paths. This fitting procedure did not include modelling of the Mo-C scattering pathways as C is a light scatterer and these C are anticipated to be relatively distant from the Mo center ($>3.7 \text{ \AA}$). All scenarios clearly show 6-coordinate Mo is formed (Figure S5), and favour 3Cl/3S coordination of the Mo center (Figures S6-S7, Table S2). These results are all consistent with the formation of the proposed $\text{Mo}^{\text{III}}(\text{ttn})\text{Cl}_3$ complex.

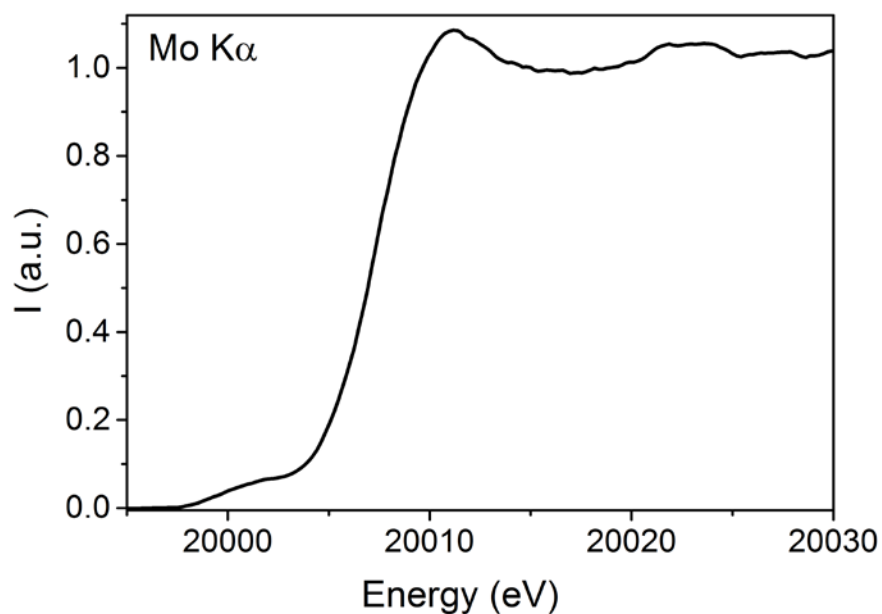


Figure S5. Normalized Mo-K α HERFD X-ray absorption spectrum of Mo^{III}(ttcn)Cl₃.

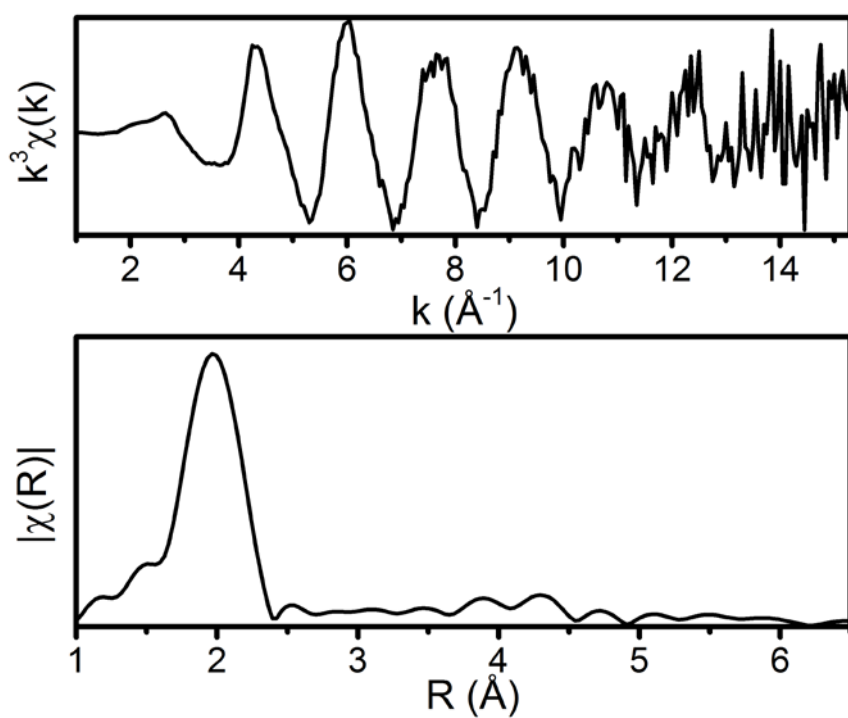


Figure S6. (top): K-space transformation of collected EXAFS of Mo^{III}(ttcn)Cl₃ weighted as k^3 . (bottom): R-space transformation of collected EXAFS of Mo^{III}(ttcn)Cl₃ for a k -range of 3.0 to 12.5 \AA^{-1} .

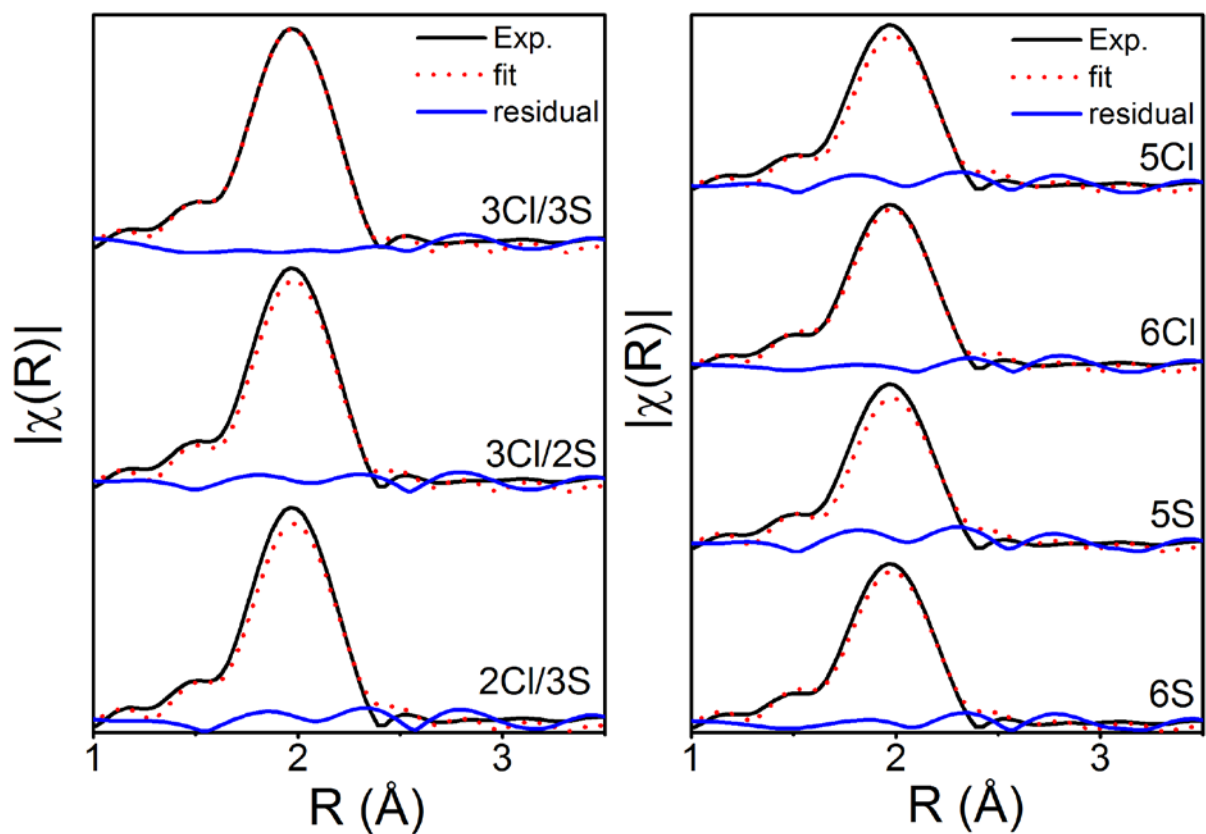


Figure S7. R-space comparison of single (Cl or S) and double (Cl and S) scattering path fits of $\text{Mo}^{\text{III}}(\text{ttcn})\text{Cl}_3$. R-space data acquired from Fourier Transform of k-space range 3 to 12.5 \AA^{-1} . Colour code: experimental spectrum (black), fitted spectrum (dotted red), residual function (blue).

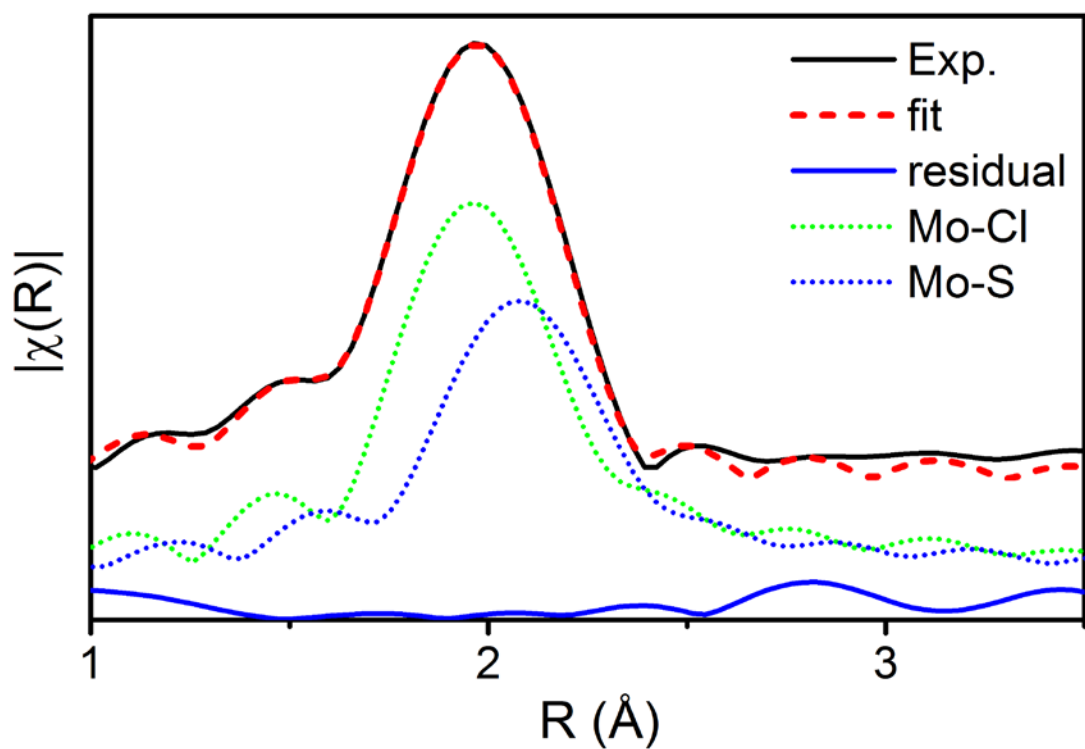


Figure S8. R-space deconvolution of 3Cl/3S model fit of Mo^{III}(ttcn)Cl₃. R-space data acquired from Fourier Transform of k-space range 3 to 12.5 \AA^{-1} . Colour code: experimental spectrum (black), fitted spectrum (dotted red), residual function (blue), spectrum of contributing Mo-Cl scattering paths (dotted green), spectrum of contributing Mo-S scattering path (dotted blue).

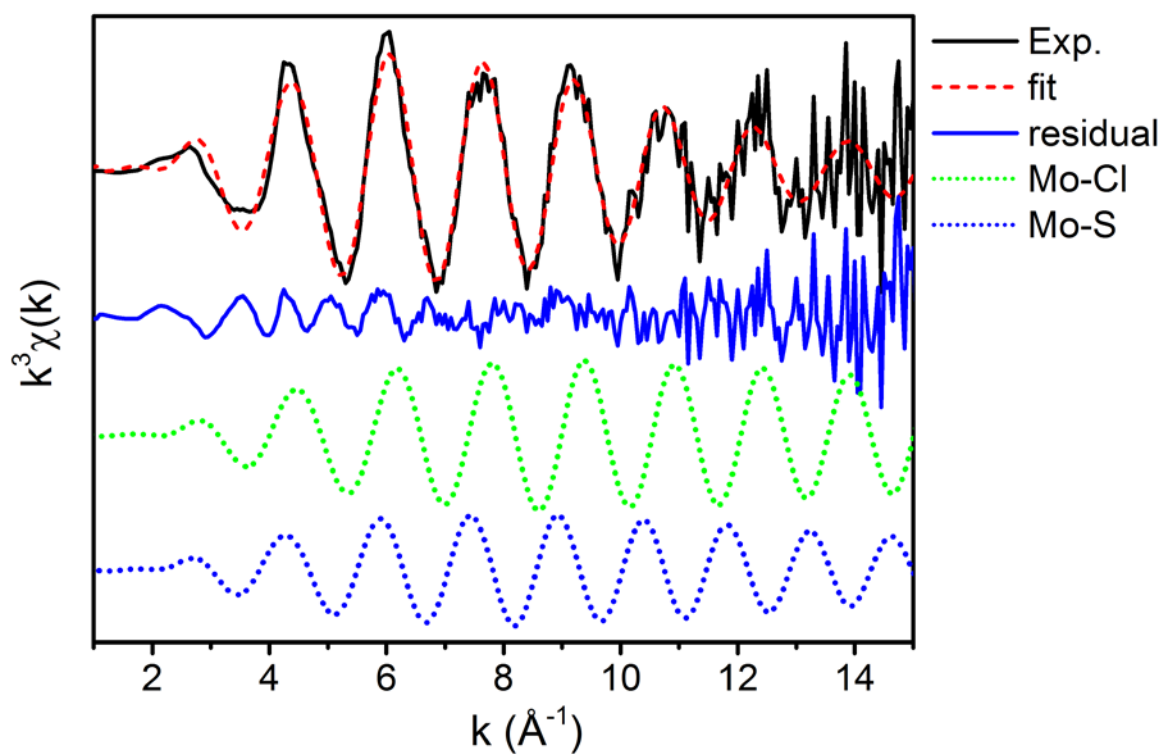


Figure S9. K-space deconvolution of 3Cl/3S model fit of $\text{Mo}^{\text{III}}(\text{tcn})\text{Cl}_3$. Colour code: experimental spectrum (black), fitted spectrum (dotted red), residual function (blue), spectrum of contributing Mo-Cl scattering paths (dotted green), spectrum of contributing Mo-S scattering path (dotted blue).

Table S2. Summary of $\text{Mo}^{\text{III}}(\text{tcn})\text{Cl}_3$ EXAFS fitting parameters. E_0 is defined as 20007.0 eV, and S_0^2 is fixed to 1.05. Fits were performed over an R range of 1 to 2.5 without phase correction. MSD (σ^2) values were restricted to lie between 0.001 and 0.005 in all fits, and do not include McMaster’s correction.

model	Path	Mo-Cl			error		
		ΔE_0	N	R	σ^2	R-factor	Reduced χ^2
3Cl/3S	Mo-Cl	4.278	3	2.403 (0.008)	0.00100 (0.00036)	0.00320	2.79
	Mo-S		3	2.515 (0.009)	0.00181 (0.00079)		
3Cl/2S	Mo-Cl	4.293	3	2.411 (0.009)	0.00100 (0.00026)	0.01410	12.30
	Mo-S		2	2.527 (0.014)	0.00100 (0.00006)		
2Cl/3S	Mo-Cl	2.840	2	2.389 (0.033)	0.00100 (0.00045)	0.01798	15.68
	Mo-S		3	2.494 (0.016)	0.00148 (0.00232)		
5Cl	Mo-Cl	4.339	5	2.443 (0.009)	0.00352 (0.00048)	0.02520	14.47
6Cl	Mo-Cl	4.272	6	2.444 (0.044)	0.00460 (0.00031)	0.00979	5.62
5S	Mo-S	1.245	5	2.452 (0.011)	0.00303 (0.00057)	0.03572	20.52
6S	Mo-S	1.196	6	2.453 (0.007)	0.00407 (0.00040)	0.01664	9.56

VI. Multiplet simulations of Mo L_3 -edge XMCD

The multiplet simulations were carried out using CTM4XAS (version 5.5), which is a crystal field approximation based package.¹³ This software utilizes the theoretical developments of Thole, Cowan and Butler.¹⁴⁻¹⁶ The Mo L_3 -edge XMCD spectra were calculated using the C_4 symmetry option in CTM4XAS in order to allow for the inclusion of an exchange field that accounts for the application of a magnetic field. Without an exchange field the XMCD signal will always be 0. The exchange field parameter was set to 100 meV. The spectra were broadened using 0.2 eV Lorentzian and 1 eV Gaussian broadening respectively. The ligand field parameters were set assuming an O_h ligand field. The splitting of the d-orbitals (10 Dq) parameter was systematically varied to see the impact of changes in ligand field on the $S=3/2$ spectrum. A tetragonal distortion was introduced (using D_s and D_t) in order to force the Mo site into an $S=1/2$ configuration. More detailed simulations are given in Figure S9 and S10, below. The calculated spectra were shifted by 2.66 eV to align with experiment.

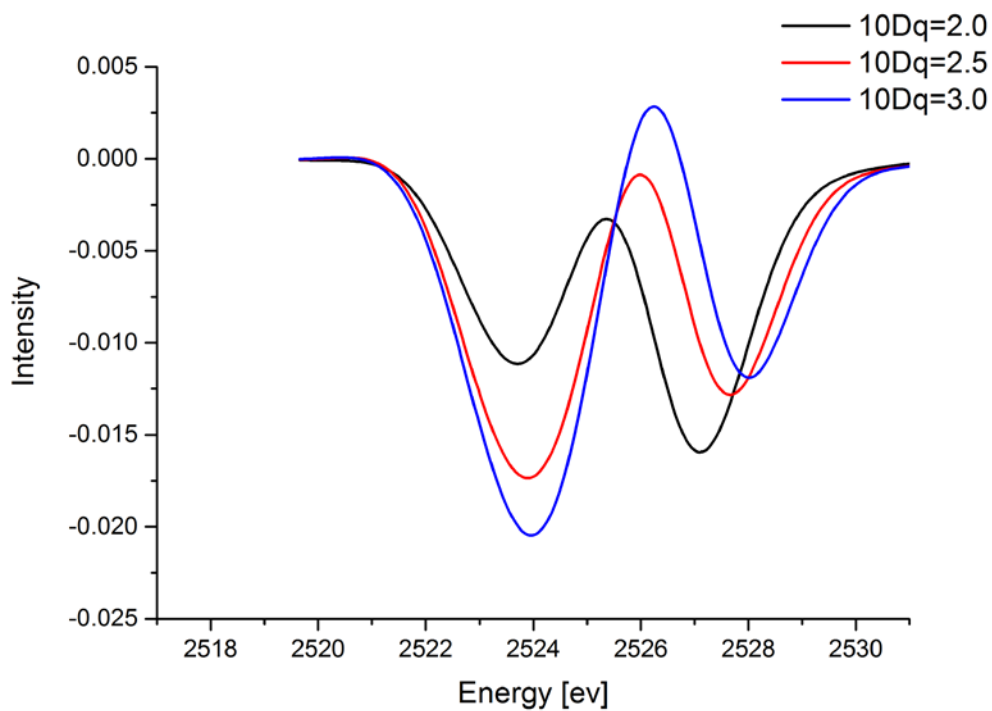
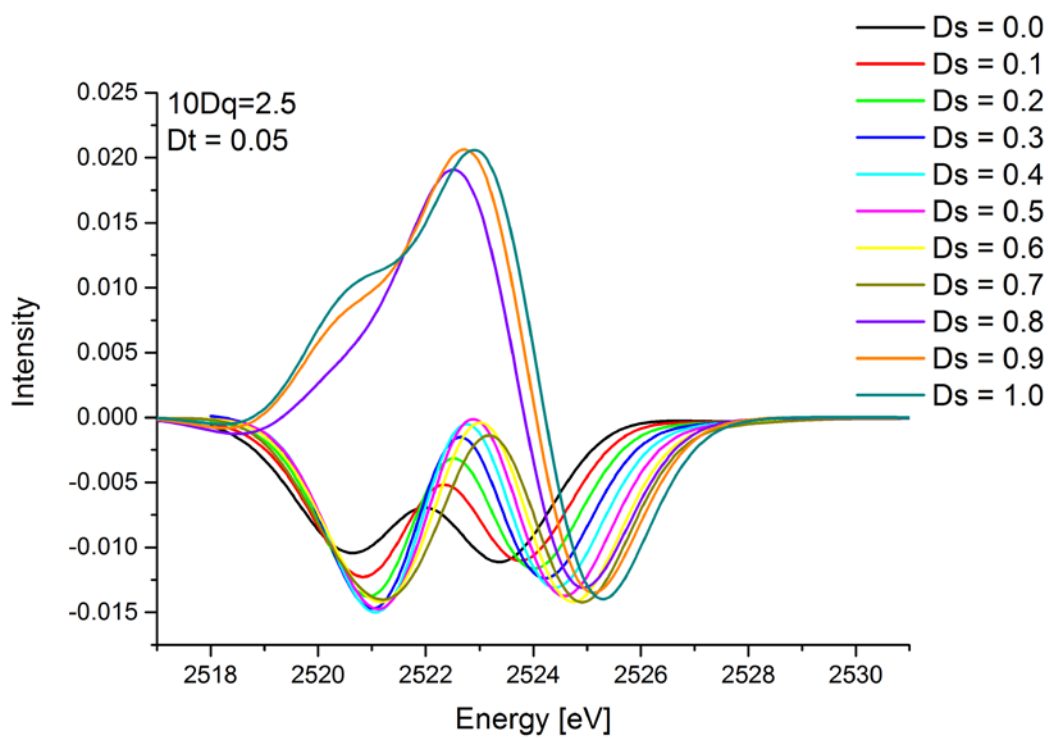


Figure S10. Multiplet calculations of Mo L₃-edge XMCD spectra of a Mo site in O_h local site symmetry with varied 10Dq values.



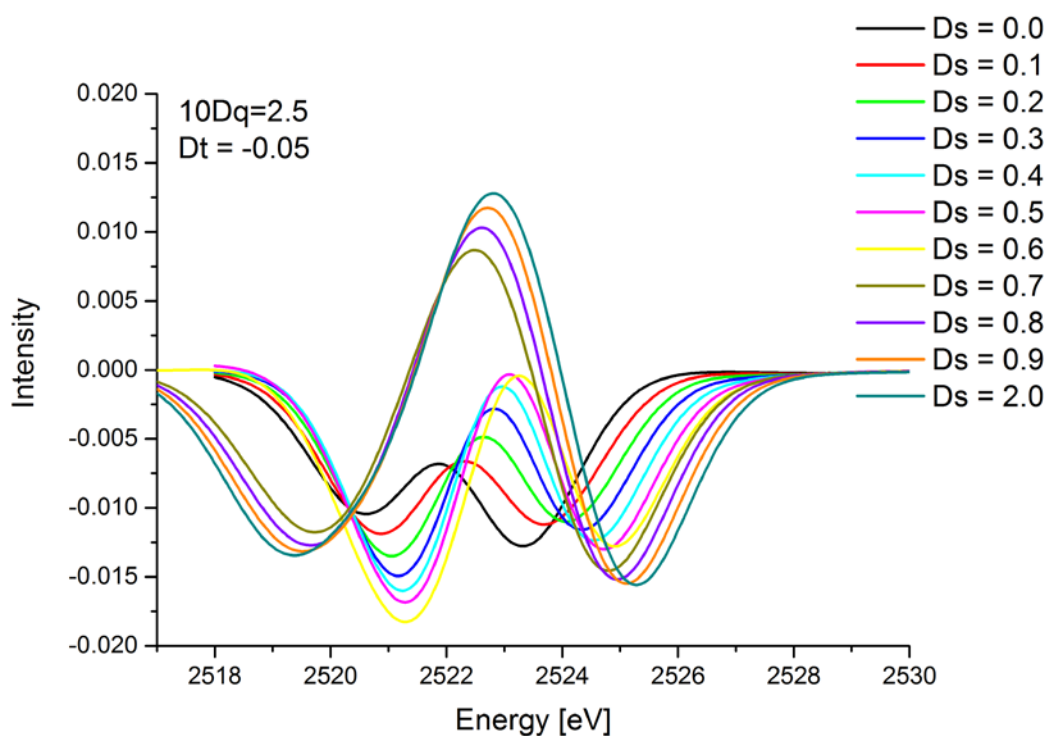


Figure S11. Multiplet calculations of Mo L₃-edge XMCD spectra of a Mo site in C₄ local site symmetry with 10Dq=2.5, D_t=0.05 on going from a high spin site (D_s values from 0.0 to 0.6) to low spin (D_s values from 0.8) (top). Note positive values of D_t indicate an axial elongation. An axial compression (negative D_t) inverts the sign of the XMCD signal from positive-negative to negative-positive. (bottom)

VII. References

1. Stoffelbach, F.; Saurenz, D.; Poli, R., Improved preparations of molybdenum coordination compounds from tetrachlorobis(diethyl ether)molybdenum(IV). *Eur. J. Inorg. Chem.* **2001**, (10), 2699-2703.
2. Fomitchev, D. V.; McLauchlan, C. C.; Holm, R. H., Heterometal cubane-type MFe₃S₄ clusters (M = Mo, V) trigonally symmetrized with hydrotris(pyrazolyl)borate(1-) and tris(pyrazolyl)methanesulfonate(1-) capping ligands. *Inorg. Chem.* **2002**, 41 (4), 958-966.
3. Spatzal, T.; Aksoyoglu, M.; Zhang, L. M.; Andrade, S. L. A.; Schleicher, E.; Weber, S.; Rees, D. C.; Einsle, O., Evidence for Interstitial Carbon in Nitrogenase FeMo Cofactor. *Science* **2011**, 334 (6058), 940-940.
4. Freeland, J. W.; Lang, J. C.; Srajer, G.; Winarski, R.; Shu, D.; Mills, D. M., A unique polarized x-ray facility at the Advanced Photon Source. *Rev. Sci. Instrum.* **2002**, 73, 1408.
5. Hedman, B.; Frank, P.; Gheller, S. F.; Roe, A. L.; Newton, W. E.; Hodgson, K. O., New Structural Insights into the Iron Molybdenum Cofactor from Azotobacter-Vinelandii Nitrogenase through Sulfur-K and Molybdenum-L X-Ray Absorption-Edge Studies. *J Am Chem Soc* **1988**, 110 (12), 3798-3805.
6. Kowalska, J. K.; Nayyar, B.; Rees, J. A.; Schiewer, C. E.; Lee, S. C.; Kovacs, J. A.; Meyer, F.; Weyhermuller, T.; Otero, E.; DeBeer, S., Iron L_{2,3}-Edge X-ray Absorption and X-ray Magnetic Circular Dichroism Studies of Molecular Iron Complexes with Relevance to the FeMoco and FeVco Active Sites of Nitrogenase. *Inorg. Chem.* **2017**, 56 (14), 8147-8158.
7. Glas, M.; Sterwerf, C.; Schmalhorst, J. M.; Ebke, D.; Jenkins, C.; Arenholz, E.; Reiss, G., X-ray absorption spectroscopy and magnetic circular dichroism studies of L1(0)-Mn-Ga thin films. *J Appl Phys* **2013**, 114 (18).

8. Ohresser, P.; Otero, E.; Choueikani, F.; Chen, K.; Stanescu, S.; Deschamps, F.; Moreno, T.; Polack, F.; Lagarde, B.; Daguerre, J. P.; Marteau, F.; Scheurer, F.; Joly, L.; Kappler, J. P.; Muller, B.; Bunau, O.; Saintavit, P., DEIMOS: A beamline dedicated to dichroism measurements in the 350-2500 eV energy range. *Rev. Sci. Instrum.* **2014**, *85* (1).
9. Ohresser, P.; Otero, E.; Choueikani, F.; Stanescu, S.; Deschamps, F.; Ibis, L.; Moreno, T.; Polack, F.; Lagarde, B.; Marteau, F.; Scheurer, F.; Joly, L.; Kappler, J. P.; Muller, B.; Saintavit, P., Polarization characterization on the DEIMOS beamline using dichroism measurements. *J. Phys. Conf. Ser.* **2013**, 425.
10. van Schooneveld, M. M.; DeBeer, S., A close look at dose: Toward L-edge XAS spectral uniformity, dose quantification and prediction of metal ion photoreduction. *J. Electron Spectrosc. Relat. Phenom.* **2015**, *198*, 31-56.
11. Sole, V. A.; Papillon, E.; Cotte, M.; Walter, P.; Susini, J., A multiplatform code for the analysis of energy-dispersive X-ray fluorescence spectra. *Spectrochim. Acta B Atomic Spectr.* **2007**, *62* (1), 63-68.
12. Ravel, B.; Newville, M., ATHENA, ARTEMIS, HEPHAESTUS: data analysis for X-ray absorption spectroscopy using IFEFFIT. *J. Synchr. Rad.* **2005**, *12*, 537-541.
13. Stavitski, E.; de Groot, F. M. F., The CTM4XAS program for EELS and XAS spectral shape analysis of transition metal L edges. *Micron* **2010**, *41* (7), 687-694.
14. Butler, P. H., *Point Group Symmetry: Applications, Methods and Tables*. Plenum Press: New York, 1981.
15. Cowan, R. T., *The Theory of Atomic Structure and Spectra*. Berkeley: University of California Press: 1981.
16. Thole, B. T.; Vanderlaan, G.; Butler, P. H., Spin-Mixed Ground-State of Fe Phthalocyanine and the Temperature-Dependent Branching Ratio in X-Ray Absorption-Spectroscopy. *Chem. Phys. Lett.* **1988**, *149* (3), 295-299.